Author's post-print (ie final draft post-refereeing) accepted for publication/published in the IEEE Transactions on Applied Superconductivity (Jun. 2020).

DOI: http://doi.org/10.1109/TASC.2020.2978036
URL: https://ieeexplore.ieee.org/document/9025061

Cite: W.-J. Yang, L. Quéval, G. Li, C.-X. Yao, G.-T. Ma, "Comparison of linear superconducting magnetic bearings using isotropic and anisotropic materials," IEEE Transactions on Applied Superconductivity, vol. 30, no. 4, id. 4901205, Jun. 2020.

Comparison of Linear Superconducting Magnetic Bearings using Isotropic and Anisotropic Materials

Wenjiao Yang, Loïc Quéval, Gang Li, Chunxing Yao, Guangtong Ma

***Abstract*—Critical current density anisotropy is a common property of high-temperature superconducting materials. We clarify here how it could impact the performances of superconducting magnetic bearings by comparing linear bearings using isotropic and anisotropic materials. To be fair, the comparison considers optimized designs. An *H*-formulation finite element model is used to obtain the levitation and guidance forces of the bearing for a given moving sequence. It is coupled with a stochastic optimization algorithm. For the considered bearing topology (single bulk above PM Halbach array), it was found that for applications requiring only levitation force, both isotropic and anisotropic materials are suitable. But for applications requiring both levitation and guidance forces, isotropic materials are more suitable than anisotropic ones since they can provide a stable guidance force for a given minimal levitation force at the smallest cost. This could serve as general design guidelines for future engineering applications.**

***Index Terms*—Superconducting magnetic bearing, anisotropy, levitation, guidance, optimization.**

I. Introduction

Linear superconducting magnetic bearing (SMB) is one of the candidate technologies for future magnetic levitation transportation [1-5]. It can provide stable levitation and guidance forces thanks to the flux trapping effect displayed by a type II superconductor cooled below its critical temperature above a permanent magnet (PM) guideway. In the past, significant efforts have been dedicated to improve the bearing topology, either by arranging the superconductors above the guideway [6], or by optimizing the PM guideway geometry [7-11]. More recently, the property of the superconductor itself started to attract attention. Several teams used 2G high-temperature superconducting (HTS) coated conductors [12-15] to take advantage of their high engineering critical current density. Our group studied to possibility of increasing the levitation force by taking advantage of the fishtail effect [16]. And Pokrovskii *et al.* explored how the anisotropy of a stack of HTS coated conductors helps improving the levitation force of an SMB by reducing the demagnetization in crossed magnetic field [17].

Another property of HTS materials can be of practical importance: the self-field critical current density anisotropy. It is usually reported that the critical current density is larger in the *ab*-plane than along the *c*-axis. Dinger *et al.* [18] used magnetization measurements and found an anisotropy ratio of 20 at 4.5 K and of 50 at 60 K in single crystals. Gyorgy *et al.* [19] obtained a similar ratio at 30 K. Selvamanickam and Salama used transport current measurements in different crystallographic directions to measure the anisotropy of the current density of YBCO bulks fabricated by the liquid phase processing method [20]. They reported an anisotropy ratio of 25 at 77 K (zero field). To take this anisotropy into account when simulating superconducting magnetic bearings, several strategies have been developed. This was either achieved by stacking multiple 2D layers [21-27], by superimposing two virtual HTS bulks [28], by considering a tensor of resistivity [29] or by using the properties of edge elements [15]. But to our best knowledge, a comparison of the performances of SMB using materials with isotropic or anisotropic critical current density has not yet been reported.

This is the goal of this work. In section II, the modeling of a linear SMB using isotropic or anisotropic materials is described. In section III, preliminary observations highlight the difficulty of performing a fair comparison and a method of evaluation is put forward. In section IV and V, both vertical and lateral displacement sequences are considered to compare the levitation and guidance performances of the SMBs.

II. Modeling

A. Superconducting magnetic bearing

The modeling of the SMB has been described in details in [30]. The PM assembly considered here is an Halbach array (Fig. 1). It is calculated with a 2D **A**-formulation (magnetostatic) finite element model. The HTS assembly is a bulk high-temperature superconductor. It is calculated with a 2D **H**-formulation finite element model. For the HTS domain, the resistivity ρ is modeled using the **E**-**J** power law model,

$$\rho(J_z) = \frac{E_c}{J_{c0}} \left| \frac{J_z}{J_{c0}} \right|^{n-1} \quad (1)$$

where J_z is the z-axis current density, J_{c0} is the critical current density, E_c is the critical current criterion and n is a material parameter. Note that the magnetic field dependence of the critical current density is neglected here. The relative movement between the HTS assembly and the PM assembly is obtained by unidirectional coupling: the sum of the magnetic field generated by the PM guideway $\mathbf{H}_{\text{ext}}$ and of the self-field generated by the

This work was supported in part by the National Natural Science Foundation of China under Grants 51722706 and 51475389 (*Corresponding author: Guangtong Ma*).

Wenjiao Yang, Gang Li, Chunxing Yao and Guangtong Ma are with the Applied Superconductivity Laboratory, State Key Laboratory of Traction Power, Southwest Jiaotong University, Chengdu 610031, China (e-mail: gtma@swjtu.edu.cn). Loïc Quéval is with the University of Paris-Saclay, CentraleSupélec, CNRS, Group of electrical engineering - Paris, 91192, Gif-sur-Yvette, France; and with Sorbonne University, CNRS, Group of electrical engineering - Paris, 75252, Paris, France (e-mail: loic.queval@centralesupelec.fr).

Color versions of one or more of the figures in this paper are available online at http://ieeexplore.ieee.org. Digital Object Identifier will be inserted here upon acceptance.

superconductor $\mathbf{H}_{\text{self}}$ is imposed as time-dependent Dirichlet boundary conditions mimicking the motion. Thanks to the adopted modeling strategy, the model is fast enough to perform optimization in a reasonable time [11]. We underline that this model has been extensively validated in [30].

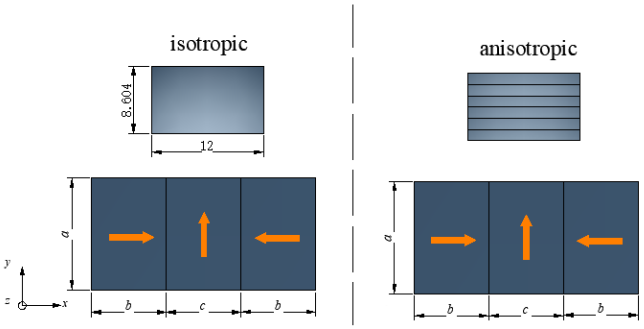

Fig. 1 - Geometry of the superconducting magnetic bearing using isotropic and anisotropic materials.

TABLE I
SUPERCONDUCTING MAGNETIC BEARING PARAMETERS

Symbol	Quantity	Value
M	PM magnetization	7.8×10^{5} A/m
E_c	Critical current criterion	1×10^{-4} V/m
n	HTS parameter	31
J_{c0}	Critical current density	4.50×10^{8} A/m^2
ρ_{air}	Air resistivity	1 Ω·m [30]
μ_0	Air/HTS permeability	$4\pi\times10^{-7}$ H/m
a	PM geometric parameter	10 mm
b	PM geometric parameter	10 mm
c	PM geometric parameter	10 mm

B. *Isotropic and anisotropic bulk*

For the isotropic material, the resistivity is assumed equal to (1) in the whole HTS domain, and a single current constraint is used to guarantee that there is no transport current,

$$\iint_{\Omega_{sc}} J_z \, \mathrm{ds} = 0 \tag{2}$$

where Ω_{sc} is the HTS domain.

For the anisotropic material, the conductivity along the *c*-axis is smaller than the conductivity in the *ab*-plane: $\sigma_c < \sigma_{a-b}$. In this work, we consider the extreme case scenario: $\sigma_c = 0$ which can be practically obtained using a stack of HTS tapes. To build such model, the bulk is divided into six subdomains. The resistivity is assumed equal to equation (1) in each subdomain. To obtain the anisotropy, each subdomain is meshed with a mapped mesh having a single element in the thickness. In addition, a current constraint similar to (2) is used in each subdomain. Note that the method to build the anisotropic HTS bulk is similar to the one used to build a homogenized model for a stack of 2G HTS coated conductors [31].

C. *Moving sequences*

The HTS bulk is liquid nitrogen cooled at a given position and then moves vertically (*y*-direction) or laterally (*x*-direction). We consider the following sequences:

- ZFC100 sequence: (a) The bulk is cooled down at a distance of 100 mm above the center of the PM guideway, where the PM guideway magnetic field can be neglected (zero field cooling). (b) The bulk is moved vertically at a speed of 1 mm/s downward until the gap between the bulk and the PM guideway is 5 mm. (c) The bulk is moved vertically upward to its initial position. This sequence is used to evaluate the levitation performance.
- FC25-LDλ sequence: (a) The bulk is cooled down at a distance of 25 mm above the center of the PM guideway. (b) The bulk is moved vertically downward until the gap between the bulk and the PM guideway is 5 mm. (c) The bulk is moved laterally first to the right at λ mm, then to the left at -λ mm, and finally back to the center. This sequence approximately reproduces the regular operation of a maglev vehicle [32]. It is used to evaluate both the levitation and guidance performances.

III. PRELIMINARY OBSERVATIONS

A. *Preliminary observations*

To underline the motivation of this work, the levitation and guidance forces of arbitrary SMBs using isotropic or anisotropic materials (Fig. 1 and Table I) are compared.

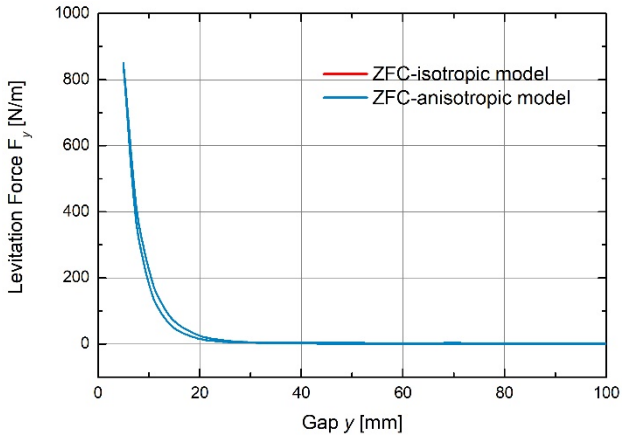

Fig. 2a - Levitation force for the ZFC100 sequence (a, b, c) = (10, 10, 10).

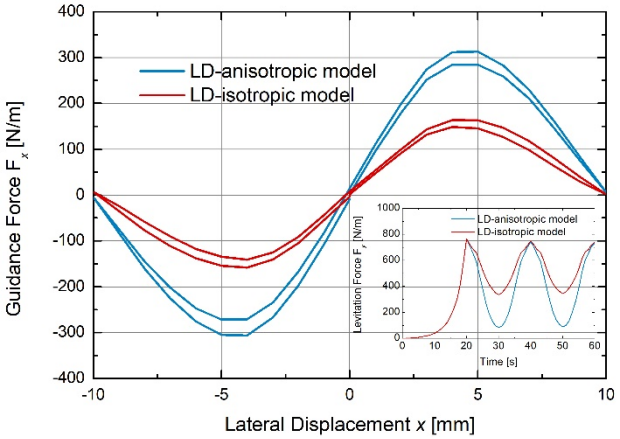

Fig. 2b - Guidance force for the FC25-LD10 sequence (a, b, c) = (10, 10, 10). Inset: Levitation force.

In Fig. 2a, the levitation force during the ZFC100 sequence is shown. It indicates that for a vertical movement, there is no difference between isotropic and anisotropic materials. This is because the induced supercurrent only flows in the *ab*-plane. Is it a generic property or does it depend on the PMG geometry?

In Fig. 2b, the levitation and guidance forces during the FC25-LD10 (λ = 10 mm) sequence are shown. It indicates that for a lateral movement, there is an important difference between isotropic and anisotropic materials. Both bearings have unstable guidance force (x<0, F_x<0), but the bearing with anisotropic material is the most unstable and its off-axis levitation force is strongly reduced in comparison with the bearing using isotropic material. Is it a generic property or does it depend on the PMG geometry? Is it possible to obtain a stable behavior? If there is a constraint on the minimal levitation force, how does the guidance forces of the bearings compare?

The above considerations suggest that it a difficult to find general guidelines based on the comparison of a single SMB.

B. *Method of comparison*

In order to draw generic conclusions, we propose here to look at the optimal PMG geometry for a given optimization problem. The dimensions of the HTS bulk are kept unchanged. The PMG is parametrized as shown in Fig. 1. During the optimization, the value of the variables *a*, *b*, and *c* can vary between 2 mm and 100 mm.

A Multi-objective Particle Swarm Optimization [33] is used in this work. The weighting factor is set at 0.8. The social and cognitive learning factors are both set at 1. The size of the swarm is set at 100 particles and >35 generations. Leaders are selected from an elitist archive.

IV. Optimal Levitation Force

A. *Objective and constraints*

We look for the PM guideways that minimize the price of the PM guideway and maximize the levitation force during the ZFC100 sequence. Accordingly, the bi-objective optimization problem can be expressed as,

$$\begin{aligned} &\text{minimize } (f_1(a, b, c), f_2(a, b, c)), \\ &\text{with } \quad f_1(a, b, c) = a\,(2b+c)\,\gamma_{PM}, \\ &\qquad f_2(a, b, c) = -F_y(t=95\ s) \end{aligned} \tag{3}$$

where the price of PM material γ_{PM} is set to 250 k€/m^3.

B. *Results and discussion*

The Pareto optimal solutions are shown in Fig. 3. In agreement with the preliminary observations, there is no difference between isotropic and anisotropic materials. Therefore, for applications requiring only levitation force, both isotropic and anisotropic materials are suitable. But the use of a stack of HTS tapes is recommended since it would have the highest engineering critical current density.

Besides, the levitation force is a logarithmic function of the cost: the slope of the Pareto front is steep at first and then decreases gradually to almost zero. This can be explained by looking at the current penetration (insets in Fig. 3). Note that the bulk it is never fully penetrated. This indicates that the quantity of HTS material could be reduced.

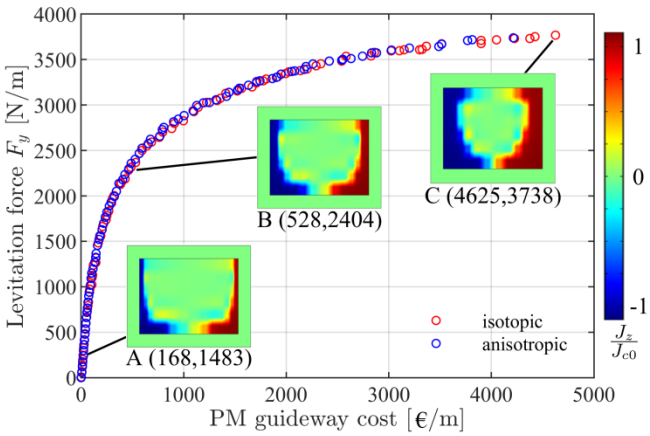

Fig. 3 - Pareto optimal solutions of the bi-objective optimization for the ZFC100 sequence. The insets show the current distributions at t = 95 s for 3 different points A, B and C along the Pareto front.

V. Optimal Guidance Force

A. *Objective and constraints*

We look for the PM guideways that minimize the price of the PM guideway and maximize the lateral force during the FC25_LDλ sequence, with a constraint on the minimum levitation force. Accordingly, the bi-objective optimization problem can be expressed as,

$$\begin{aligned} &\text{minimize } (f_1(a, b, c), f_2(a, b, c)), \\ &\text{subject to } \quad c_1(a, b, c) < 0, \\ &\text{with } \quad f_1(a, b, c) = a\,(2b+c)\,\gamma_{PM}, \end{aligned} \tag{4}$$

$$f_2(a, b, c) = -F_x\,(t=20+3\lambda\ s),$$

$$c_1(a, b, c) = \delta - \min\,(F_y(t>20\ s))$$

where δ is the minimum levitation force constraint.

B. Results and discussion

The Pareto optimal solutions for the FC25-LD10 sequence ($\lambda = 10$ mm) with a minimum levitation force set to 250 N are shown in Fig. 4. The guidance force is also a logarithmic function of the cost. And the bearing with isotropic material offers a larger guidance force than the one with anisotropic material. According to equation (4), the guidance force is evaluated when the lateral displacement is equal to -10 mm. For this permanent guideway topology and for this sequence, the optimal guidance force obtained with the isotropic model is always positive while the one obtained from the anisotropic model is almost always negative. Therefore the optimal bearing with isotropic material is always stable (x<0, F_x>0) while the one with anisotropic material is almost always unstable (x<0, F_x<0). Note that this is in agreement with the measurements reported in [15] (Fig. 9), in which we measured an unstable guidance force for a stack of HTS tapes for same sequence.

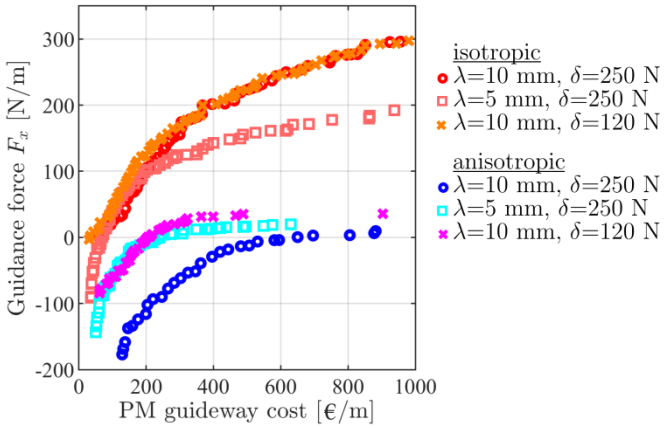

Fig. 4 - Pareto optimal solutions of the bi-objective optimization for the FC25-LDλ sequence for various combinations of the lateral displacement amplitude λ and of the levitation force constraint δ.

Before drawing a generic conclusion, we look at the impact of the lateral displacement amplitude λ and of the levitation force constraint δ.

First, we decrease the lateral displacement amplitude. The Pareto optimal solutions for the FC25-LD5 sequence ($\lambda =$ 5 mm) with a minimum levitation force set to 250 N have been added to Fig. 4. The bearings with isotropic material are now unstable (x<0, F_x<0) at low cost, and stable (x<0, F_x>0) at high cost. For a smaller lateral displacement, one must spend more to obtain the same guidance force as before. And the anisotropic model is still hardly stable (x<0, F_x>0).

Second, we decrease the levitation force constraint. The Pareto optimal solutions for the FC25-LD10 sequence ($\lambda =$ 10 mm) with a minimum levitation force set to 120 N are also shown in Fig. 4. By decreasing the required levitation force to δ=120 N, the anisotropic model can now be stable (x<0, F_x>0) at a lower cost than with δ=250 N. This feature has not been reported before. This underlines that for a bearing with anisotropic material, the levitation and guidance performance are two conflicting objectives.

We underline that, for a given cost, the guidance force of the bearings with anisotropic material is always much lower than the one of the bearing with isotropic material. Besides, even for a large cost, the guidance force of bearings with anisotropic materials stays small. Therefore, for applications requiring both levitation and guidance forces, anisotropic materials might be unsuitable.

VI. CONCLUSION

In this work, the levitation and guidance performances of linear superconducting magnetic bearings with isotropic or anisotropic critical current density materials have been compared. As the performance of a bearing depends on the geometry of the PM guideway, it's hard to draw a general conclusion with one given PM guideway. To deal with this issue, we proposed to solve an optimization problem. This allowed us to compare two different bearings (one using isotropic material and the other using anisotropic material) for a given set of requirements (topology, moving sequence, minimum force, etc.).

For the adopted bearing topology (Halbach array PM guideway and single HTS bulk), we could draw the following general conclusions. For applications requiring only levitation force, both isotropic and anisotropic materials are suitable since they have the same Pareto optimal solutions. The use of a stack of HTS tapes is recommended since it has the highest engineering critical current density. For applications requiring both levitation and guidance forces, isotropic materials are more appropriate since they can generally provide a stable guidance force for a given minimal levitation force at the smallest cost. We underline that anisotropic materials can provide a guidance force as well if the constraint on the minimal levitation force is low, but its value is generally quite small.

REFERENCES

[1] J. Wang *et al.*, "The first man-loading high temperature superconducting Maglev test vehicle in the world," *Phy. C: Supercond.*, vol. 378, no. 2, pp. 809-814, Oct. 2002.

[2] Z. Deng *et al.*, "A high-temperature superconducting maglev ring test line developed in Chengdu, China," *IEEE Trans. Appl. Supercond.*, vol. 26, no. 6, id. 3602408, Sep. 2016.

[3] L. Schultz *et al.*, "Superconductively levitated transport system - the SupraTrans project," *IEEE Trans. Appl. Supercond.*, vol. 15, no.2, pp. 2301-2305, Jun. 2005.

[4] C. Beyer, O. de Haas, P. Verges, L. Schultz, "Guideway and turnout switch for the SupraTrans project," *J. Phys.: Conf. Ser.*, vol. 43, pp. 991-994, 2006.

[5] G.G. Sotelo, D.H.N Dias, R.A.H. de Oliveira, A.C Ferreira, R. de Andrade, Jr., R.M. Stephan, "MagLev Cobra: test facilities and operational experiments," *J. Phys.: Conf. Ser.*, vol. 507, no. 3, id. 032017, 2014.

[6] Z. Deng, D. He, J. Zheng, "Levitation performance of rectangular bulk superconductor arrays above applied permanent-magnet guideways," *IEEE Trans. Appl. Supercond.*, vol. 25, no. 1, id. 3600106, Feb. 2015.

[7] J. Zhang, Y. Zeng, J. Cheng, X. Tang, "Optimization of permanent magnet guideway for HTS Maglev vehicle with numerical methods," *IEEE Trans. Appl. Supercond.*, vol. 18, no. 3, pp. 1681-1686, Sep. 2008.

[8] N. Del-Valle, A. Sanchez, C. Navau, D.-X. Chen, "Theoretical hints for optimizing force and stability in actual Maglev devices," *IEEE Trans. Appl. Supercond*., vol. 19, no. 3, pp. 270-273, Jun. 2009.

[9] G.G. Sotelo, D.H.N. Dias, R. de Andrade, Jr., R.M. Stephan, "Tests on a superconductor linear magnetic bearing of a full-scale Maglev vehicle," *IEEE Trans. Appl. Supercond*., vol. 21, no. 3, pp. 1464-1468, Jun. 2011.

[10] E.S. Motta *et al*., "Optimization of a linear superconducting levitation system," *IEEE Trans. Appl. Supercond*., vol. 21, no. 5, pp. 3548-3554, Oct. 2011.

[11] L. Quéval, G.G. Sotelo, Y. Kharmiz, D.H.N. Dias, F. Sass, V.M.R. Zermeño, R. Gottkehaskamp, "Optimization of the superconducting linear magnetic bearing of a maglev vehicle," *IEEE Trans. Appl. Supercond.*, vol. 26, no. 3, id. 3601905, Apr. 2016.

[12] F. Sass, G.G. Sotelo, A. Polasek, R. de Andrade, Jr., "Application of 2G-tape for passive and controlled superconducting levitation" *IEEE Trans. Appl. Supercond*., vol. 21, no. 3, pp. 1511-1514, Feb. 2011.

[13] S. Samoilenkov *et al.*, "Customised 2G HTS wire for applications," *Supercond. Sci. Technol.*, vol. 29, no. 2, id. 024001, Dec. 2016.

[14] A. Patel, S.C. Hopkins, A. Baskys, V. Kalitka, A. Molodyk, A.B. Glowacki, "Magnetic levitation using high temperature superconducting pancake coils as composite bulk cylinders," *Supercond. Sci. Technol*., vol. 28, no. 11, id. 115007, Sep. 2015.

[15] K. Liu, W. Yang, G.-T. Ma, L. Quéval, T. Gong, C. Ye, X. Li, Z. Luo, "Experiment and simulation of superconducting magnetic levitation with REBCO coated conductor stacks," *Supercond. Sci. Technol.*, vol. 31, no. 1, id. 015013, Dec. 2017.

[16] Z.-Y. Yan, W.-J. Yang, C.-Q. Ye, R.-C. Wang, L. Quéval, G. Li, K. Liu, G.-T. Ma, "Numerical prediction of levitation properties of HTS bulk in high magnetic fields," *IEEE Trans. Appl. Supercond.*, vol. 29, no. 5, id. 3602805, Aug. 2019.

[17] S. Pokrovskii, M. Osipov, D. Abin, I. Rudnev, "Magnetization and levitation characteristics of HTS tape stacks in crossed magnetic fields," *IEEE Trans. Appl. Supercond.*, vol. 26, no. 3, id. 8201304, Apr. 2016.

[18] T.R. Dinger, T.K. Worthington, W.J. Gallagher, R.L. Sandstrom, "Direct observation of electronic anisotropy in single-crystal $Y_1Ba_2Cu_3O_{7-x}$," *Phys. Rev. Lett.*, vol. 58, p. 2687, Jun. 1987.

[19] E.M. Gyorgy, R.B. van Dover, K.A. Jackson, L.F. Schneemeyer, J.V. Waszczak, "Anisotropic critical currents in $Ba_2YCu_3O_7$ analyzed using an extended Bean model," *Appl. Phys. Lett.*, vol. 55, no. 3, pp. 283-285, Dec. 1989.

[20] V. Selvamanickam, K. Salama, "Anisotropy and intergrain current density in oriented grained bulk $YBa_2Cu_3O_x$ superconductor," *Appl. Phys. Lett.*, vol. 57, no. 15, pp. 1575-1577, Jul. 1990.

[21] H. Ueda, S. Azumaya, S. Tsuchiya, A. Ishiyama, "3D electromagnetic analysis of levitating transporter using bulk superconductor," *IEEE Trans. Appl. Supercond*., vol. 16, no. 2, pp. 1092-1095, Jun. 2006.

[22] X.-J. Zheng, Y. Yang, "Transition cooling height of high-temperature superconductor levitation system." *IEEE Trans. Appl. Supercond*., vol. 17, no. 4, pp. 3862-3866, Dec. 2007.

[23] M. Uesaka, Y. Yoshida, N. Takeda, K. Miya, "Experimental and numerical analysis of three-dimensional high-Tc superconducting levitation systems," *Int. J. Appl. Electromagn. Mater.*, vol. 4, pp. 13-25, 1993.

[24] Y. Yoshida, M. Uesaka, K. Miya, "Magnetic field and force analysis of high Tc superconductor with flux flow and creep," *IEEE Trans. Magn.*, vol. 30, no. 5, pp. 3503-3506, Sep. 1994.

[25] M. Tsuchimoto, T. Honma, "Numerical evaluation of levitation force of HTSC flywheel," *IEEE Trans. Magn*., vol. 4, no. 4, pp. 211-215, Dec. 1994.

[26] M. Tsuda, H. Lee Y. Iwasa, "1998 Electromaglev (active-maglev)-magnetic levitation of a superconducting disk with a DC field generated by electromagnets: III. Theoretical results on levitation height and stability," *Cryogenics*, vol. 38, no. 7, pp. 743-756, 1998.

[27] M. Tsuda, H. Lee, S. Noguchi, Y. Iwasa, "Electromaglev (active-maglev)-magnetic levitation of a superconducting disk with a DC field generated by electromagnets: IV. Theoretical and experimental results on supercurrent distributions in field-cooled YBCO disks," *Cryogenics*, vol. 39, pp. 893-903, 1998.

[28] Y.-Y. Lu, J.-S. Wang, S.-Y. Wang, J. Zheng, "3D-modeling numerical solutions of electromagnetic behavior of HTSC bulk above permanent magnetic guideway," *J. Supercond. Nov. Magn.*, vol. 21, no. 8, pp. 467-474, Dec. 2008.

[29] G.-T. Ma, J.-S. Wang, S.-Y. Wang, "3D modeling of high-Tc superconductor for magnetic levitation/suspension application: I. Introduction to the method," *IEEE Trans. Appl. Supercond.*, vol. 20, no. 4, pp. 2219-2227, Apr. 2010.

[30] L. Quéval, K. Liu, W. Yang, V.M.R. Zermeño, G.-T. Ma, "Superconducting magnetic bearings simulation using an H-formulation finite element model," *Supercond. Sci. Technol.*, vol. 31, no. 8, id. 084001, Jun. 2018.

[31] V.M.R. Zermeño, A.B. Abrahamsen, N. Mijatovic, B.B. Jensen, M.P. Sørensen, "Calculation of alternating current losses in stacks and coils made of second generation high temperature superconducting tapes for large scale applications," *J. Appl. Phys.*, vol. 114, no. 17, id. 173901, Nov. 2013.

[32] G.G. Sotelo *et al.*, "Tests with one module of the Brazilian Maglev-Cobra vehicle," *IEEE Trans. Appl. Supercond.*, vol. 23, no. 3, id. 3601204, Jun. 2013.

[33] J. Aubry, "Optimisation du dimensionnement d'une chaîne de conversion électrique directe incluant un système de lissage de production par supercondensateurs: application au houlogénérateur SEAREV," (in French), Ph.D. dissertation, Ecole Normale Supérieure Cachan, Cachan, France, 2011. [Online]. Available : https://hal.archives-ouvertes.fr/tel-00662488